Understanding the Enhancement of Surface Diffusivity by Dimerization

C. Zaum[1] and K. Morgenstern[2]

[1]*Leibniz Universität Hannover, ATMOS, Appelstrasse 2, D-30167 Hannover, Germany*
[2]*Ruhr-Universität Bochum, Physikalische Chemie I, D-44780 Bochum, Germany*

Beyond dilute coverage, the collective diffusion of molecules might enhance material transport. We reveal an enhanced mobility of molecular dimers by separating two motions, diffusion and rotation, of CO dimers on elemental Ag(100) as well as on a dilute Cu alloy of Ag(100). From time-lapsed scanning tunneling microscopy movies recorded between 15 and 25 K, we determine the activation energy of dimer diffusion on elemental Ag(100) to be, at (40 ± 2) meV, considerably smaller than the one for monomer diffusion, at (72 ± 1) meV. The alloyed Cu atoms reduce the dimer mobility facilitating to determine their rotational barrier separately to be (39 ± 3) meV. Disentangling different degrees of freedom suggests that a rotational motion is at the origin of enhanced dimer diffusivity.

A variety of basic physical and chemical processes start with the transport of particles on a surface. For this reason, diffusion of elemental atoms on homogeneous surfaces is well studied [1]. For molecular adparticles [2], processes affected by molecular diffusion include self-organization of supramolecular structures and surface reactions in heterogeneous catalysis, where the diffusion of the reactants to the reactive sites on the surface is an essential and often rate-determining step [3]. In this respect, CO, as constituent of CO oxidation, is considered as a model molecule for molecular motion [4].

Most diffusion studies investigate individual adparticles or dilute coverages at which adparticles do not interact [1]. Though providing important fundamental information, such studies might not give the full picture of the influence of adparticle diffusion on the abovementioned processes, during which particle interaction is frequent. In fact, three studies reported a major increase of molecular diffusivity upon dimer formation, for CO on Cu(110) [5], water on Pd(111) [6], and tetra-pyridylporphyrin on Cu(111) [7]. The understanding of this increase is limited only. Only the increased diffusivity for water dimers was explained theoretically [8]. There, the activation barrier is reduced by hydrogen bond rearrangements facilitating hydrogen tunneling as a diffusion step. Such a hydrogen tunneling is not possible for the other two cases.

On the other hand, extended objects as atom clusters or organic molecules revealed higher complexity in surface diffusion than hopping motion between neighboring adsorption sites. For instance, long jumps are involved in the motion of decacyclene and hexa-tert-butyl deca-cyclene on Cu(110) [9] and *n*-butane on Pt(111) and Cu(100) [10]. The large prefactor of C_{60} diffusion on Pd(100) indicated a rolling motion of this spherical molecule [11]. Three studies pointed to an importance

of rotational motion for the diffusion of extended objects. The collective slip-diffusion motion of Au_{140} nanoclusters on graphite involves a correlation of rotational motion with lateral translation [12]. Tris(2-phenylpyridine)iridium (III) [Ir(ppy)3] showed both translational and rotational transitions on Cu(111) [13]. A theoretical analysis of Co-phthalocyanine diffusivity on Ag(100) revealed a combined translational and rotational molecular motion [14].

In this Letter, we report an increased mobility of CO dimers on Ag(100) as compared to monomers. We separate the translational and rotational motions of CO dimers by comparing their diffusion on an elemental surface to the one on a dilute surface alloy of Cu in Ag(100). The stronger adsorption of one of the CO molecules to a Cu atom hinders the long-range diffusion of CO dimers, allowing us to determine the rotational energy barrier. Our study thus identifies the additional degree of rotational freedom to increase dimer mobility of CO on Ag(100).

STM measurements are performed with a low-temperature STM under ultrahigh vacuum conditions [15]. The Ag(100) surface is cleaned by standard cycles of sputtering and annealing. For formation of the surface alloy, a few percent of a monolayer of copper is deposited at room temperature and postannealed as described in Ref. [16]. CO is deposited on both surfaces at 22 K.

The kinetics of the molecules is followed in time-lapse series (called movies), for which the same spot on the surface is repeatedly scanned at predetermined time intervals. We follow the analysis procedure originally developed for field ion microscopy studies as summarized in Ref. [1] applied to STM [17]. The precision of the energy barriers and prefactors determined from Arrhenius plots depends crucially on the precision of the temperature measurement at the sample surface. We use the procedure and analysis outlined in Ref. [17] to determine the
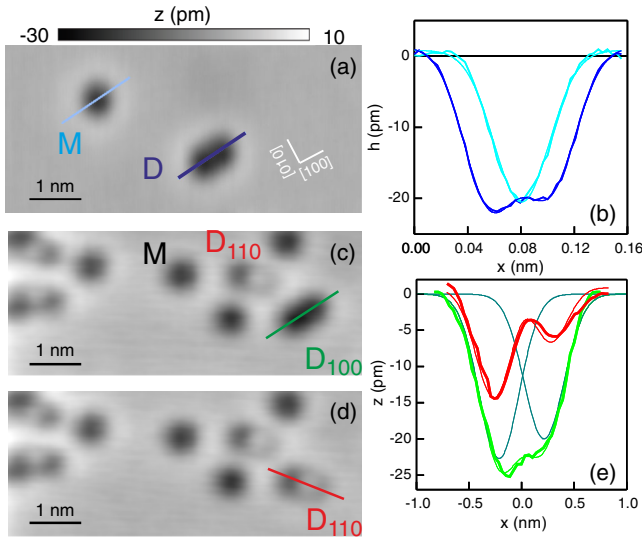
FIG. 1.   Identification of CO monomers M and dimers D on (a), (b) Ag(100) and on (c)–(e) 2%Cu/Ag(100) surface alloy: (a) STM image, 44 pA, 50 mV, 16 K; (b) height profile across monomer (blue) and dimer (dark blue) with Gaussian fits (thin lines). (c),(d) Two snapshots of movie, $\Delta t = 285$ s (20 pA, 50 mV, 16 K); $\langle 100 \rangle$-oriented dimer (D_{100}), and $\langle 110 \rangle$-oriented dimer (D_{110}) marked. (e) Line profiles along lines in (c),(d) with fit of D_{100} (green) by two negative Gaussian profiles (blue); fit of the D_{110} dimer profile by the D_{100} profile and an additional positive Gaussian profile (red).

temperature with subkelvin precision. For further details, see Ref. [18].

Here we investigate the structures shown in Fig. 1, where identification of the dimers involves manipulation experiments; see Ref. [18]. Monomers known to bind to on-top sites on metal surfaces are imaged on both surfaces as depressions; on Ag(100) with an apparent depth of (22.0 ± 0.2) pm in the probed voltage and current range [Figs. 1(a) and 1(b)]. Dimers on Ag(100) imaged as elliptically shaped depressions consist of two CO molecules adsorbed on next-nearest-neighboring sites in the Ag$\langle 100 \rangle$ direction with similar apparent depths at (20.1 ± 0.4) and (20.8 ± 0.4) pm [Fig. 1(b)]. Their center of mass is situated above a surface hollow site [18].

Cu atoms in the surface alloy display a typical apparent depth of ≈ 6 pm at most voltages; see Refs. [16,18,20]. CO binds preferentially to these alloyed Cu atoms as such depressions disappear upon CO adsorption. Structures consisting of either two adjacent depressions in the $\langle 100 \rangle$ direction (marked D_{100}) or a chain consisting of a depressions, a local protrusion, and a depression of smaller depth in the $\langle 110 \rangle$ direction [D_{110}, Figs. 1(c) and 1(d)] are identified as dimers [18]. D_{100} is a dimer that consists of two molecules adsorbed on next-neighboring surface sites along $\langle 100 \rangle$, where a small difference in apparent depth indicates that the two molecules are adsorbed on two different atoms [Fig. 1(e)]. D_{110} is a dimer with two
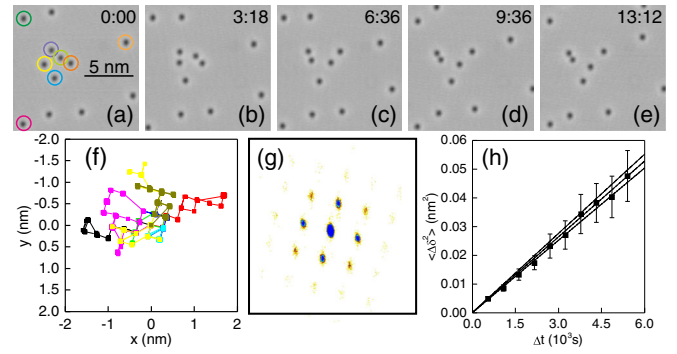

FIG. 2.   Monomer diffusion on Ag(100). (a)–(e) Snapshots of a movie, 21.8 K, $\Delta t = 540$ s, 44 pA, 50 mV; time in h:min; snapshots are cutouts of the original image size for better visibility. (f) Track of monomers marked in (a). (g) Jump distance distribution at 22.8 K, $N_{\text{tot}} = 25668$. (h) Einstein plot; $\delta = x$ or y; linear fit yields $D = (4.4 \pm 0.2) \times 10^{-6}$ nm^2/s.

molecules adsorbed in neighboring surface sites along $\langle 100 \rangle$, with one of the molecules tilted, giving rise to a local protrusion between the two depressions [Fig. 1(e)].

Diffusion is followed in image series as shown in Figs. 2(a)–2(e) for the elemental surface. For a visual impression, see Ref. [18]. The CO monomers jump between lattice sites as evidenced by the track of the molecules [Fig. 2(f)] and the jump distance distribution [Fig. 2(g)].

We now normalize each measured position to these lattice sites and derive the diffusivities in the x and y directions from the jump distance distributions in Fig. 2(g). This analysis shows that the motion is symmetric and independent in the two directions. The diffusivities follow the Einstein relation $\langle \Delta \delta^2 \rangle = 2D\Delta t$ with $\delta = x$ or y confirming a random motion [Fig. 2(h)].

Dimer motion is followed in two temperature ranges. Between 22 and 24 K, the dimers form spontaneously from diffusing monomers. For extending this temperature range, we form dimers between 15 and 17 K by lateral force manipulation. In the intermediate temperature range, monomers are too mobile to facilitate manipulation but too immobile to spontaneously form dimers.

Diffusion in the lower temperature range is exemplified at $T = 15.5$ K in Figs. 3(a)–3(e). At the higher temperature, the dimer moves larger distances in smaller time intervals [Fig. 3(f)]. Also, the dimer moves only by lattice site distances [track in Fig. 3(g) and jump distance distribution in Fig. 3(h)]. Its diffusion is symmetric and independent in x and y [Fig. 3(h)] and follows the Einstein relation.

The temperature-dependent diffusivities D for monomer and dimer diffusion are extracted via the Einstein relation and displayed half-logarithmically versus the inverse temperature in Fig. 4(a). In view of the clear Arrhenius behavior, the diffusion barrier E_D is determined from the measured diffusivities D at temperatures T via [1]
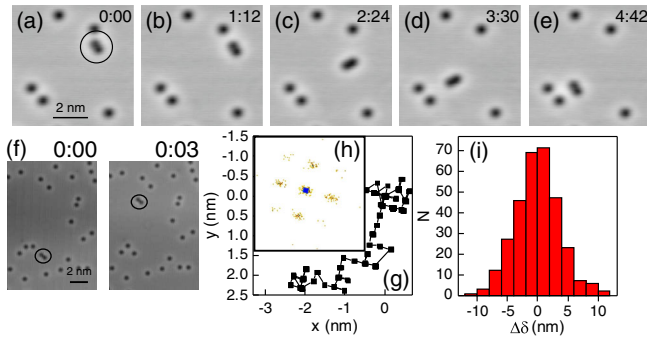
FIG. 3. Dimer diffusion on Ag(100), time in h:min. (a)–(e) Snapshots of movie recorded at 15.5 K, $\Delta t = 90$ s, 44 pA, 50 mV. (f) Two images of movie at 22.8 K, 50 mV, 44 pA; dimer marked by circle. (g) Track of dimer marked in (a). (h) Jump distance distribution at 15.5 K, $N_{tot} = 623$. (i) Jump distance histogram from movie recorded at 22.8 K. $\delta = x$ or y.

$$D = D_0 e^{-E_D/kT} \quad \text{with} \quad D_0 = \frac{N_{\text{sites}}}{2N_{\text{dim}}} a^2 \nu_0 e^{\Delta S_D/k}, \quad (1)$$

with prefactor D_0, Boltzmann constant k, dimensionality of the motion N_{dim}, number of possible diffusion directions N_{sites}, surface lattice a, and entropy difference between ground and transition state ΔS_D. It yields $E_D^{\text{mon}} = (72 \pm 1)$ meV and $E_D^{\text{dim}} = (40 \pm 2)$ meV [Fig. 4(a)], a substantial decrease in activation energy upon dimerization.

The prefactor determined for the monomer $D_0^{\text{mon}} = 1.9 \times 10^{11\pm0.3}$ nm^2/s corresponds to a negligible entropy difference $\Delta S_D = (0.03 \pm 0.16)$ meV/K according to Eq. (1) using $a = 0.289$ nm, $N_{\text{dim}} = 2$, and $N_{\text{sites}} = 4$
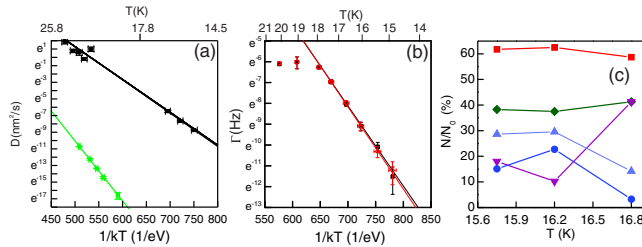

FIG. 4. (a),(b) Arrhenius plots: (a) Diffusion of CO monomers (green circles) and dimers (black squares) on Ag(100) with linear fits yielding $E_D^{\text{mon}} = (72 \pm 1)$ meV and $D_0^{\text{mon}} = 1.9 \times 10^{11\pm0.3}$ nm^2/s and $E_D^{\text{dim}} = (40 \pm 2)$ meV and $D_0^{\text{dim}} = 1.9 \times 10^{9\pm0.6}$ nm^2/s; (b) configurational change of CO dimers on Cu/Ag(100) from the D_{110} dimer to the D_{100} dimer (black filled squares) and back (red open circles); linear fits yield $E_D = (38 \pm 2)$ meV and $\Gamma_0 = 2.97 \times 10^{8.0\pm0.7}$ Hz (red line) and $E_D = (39 \pm 2)$ and $\Gamma_0 = 1.23 \times 10^{8.0\pm0.7}$ Hz (black line). The three points at $T > 17.5$ K are not considered for curve fitting. (c) Percentage of different types of dimer motion on an elemental surface. Red squares: all events with change in orientation; green diamonds: only diffusion; blue up triangles: only motion around one monomer; dark blue circles: only rotation around center of dimer; purple down triangles: both diffusion and rotation; $N_0 (15.8\,K) = 247$; $N_0(16.2\,K) = 88$; $N_0(16.8K) = 622$.

for the quadratic Ag(100). Thus, the monomer diffusion is similar to atomic diffusion without any entropy difference between the ground and the transition state. In contrast, the prefactor determined for the dimer $D_0^{\text{dim}} = 1.9 \times 10^{9\pm0.6}$ nm^2/s corresponds to an entropy change of $\Delta S_D = -(0.41 \pm 0.24)$ meV/K, which points to a reduction of one additional degree of freedom in the transition state according to transition state theory. The Meyer-Nedel compensation law predicts a reduction in the prefactor with energy, e.g., for Cu monomers and dimers diffusing on Cu(100) [23]. However, this law explains only a few percent changes and not orders of magnitude as observed here. The origin of the problem lies in intrinsic correlations between the energy and prefactor, which make it hard to separate the two. Note that STM is only able to determine diffusivities in a limited temperature interval. Thus, extrapolated prefactors have larger uncertainties than energies. Assuming the monomer's prefactor to be the correct one, it is possible to fit the dimer data at a slightly enhanced energy, i.e., (48 ± 2) meV, still much smaller than the diffusion energy of the monomer. We note that other experimental data on dimer diffusion are likewise consistent with equivalent prefactor and different energy barriers; e.g., Refs. [5,7]. The reduction in energy is thus an important result independent of the exact determination of the prefactor or small changes in entropy and not restricted to our specific sample, which we attempt to understand in the following.

For dimer formation of Cu on Ag(111), a decrease in diffusion barrier (from 73 to 65 meV) was explained via comparison to theoretical calculations by a loss in commensurability [24–27]. For metallic atoms, the lateral displacement is too small to be detectable by STM [26]. In contrast, the imaging of CO is much more sensitive to the exact orientation of the molecular axis and its position on a surface [21,28]. Our high-resolution images do not give any indication of such a change upon binding, presumably because the binding energy between two CO molecules is much weaker than between metallic atoms. Indeed, in gas phase the attractive energy minimum at a molecule distance of 380 pm is only 10 meV [22]. Density functional theory (DFT) calculations are not even able to stabilize the dimer on Ag(100) [29]. It is thus unlikely that registry effects cause the reduction in energy barrier.

The dimer changes between two rotational orientations during diffusion [Figs. 3(a)–3(e)]. We propose this rotational motion to be at the origin of the reduced energy barrier.

To prove our point, we recall that an inhomogeneous distribution of Pb atoms in a Cu surface alloy reduces the diffusion rate of Cu adatoms [30]. Here we reduce the mobility of the CO dimers by alloying Cu into Ag(100) [16,20]. Indeed, in the temperature range of CO diffusion on elemental Ag(100), the dimers bound to Cu atoms show no long-range diffusivity. However, they frequently change their orientation and rotate around a Cu atom (Fig. 5). We are thus able to determine the activation energy for the

dimer rotation. To this aim, we determine separately the jump rates Γ from the D_{110} to the D_{100} dimer and back between 15 and 21 K. In the Arrhenius plot, these two data sets follow a straight line up to 18 K, as expected for an activated motion [Fig. 4(b)]. Above this temperature, the data points level off, because at higher temperature the orientation changes on the timescale of image acquisition; not all changes are observed. By calculating these events, the other points fall on a straight line also (not shown). The fits yield identical values well within the error bars, regardless of whether these corrected data or only the data at lower temperature are fitted. The activation energy is $E_D = (38 \pm 2)$ meV for a change from D_{110} to D_{100} and $E_D = (39 \pm 2)$ meV for the opposite motion. The two processes are thus symmetric.

The energy barrier of dimer rotation on alloyed Ag(100) is at (38 ± 2) meV within the error bars of dimer rotation on elemental Ag(100) at (39 ± 3) meV. This coincidence suggests that the reduced diffusion barrier on the elemental surface results from a sequence of rotational motions, a motion much lower in energy than the monomer hopping motion. But are rotations identical on the alloy and on the elemental surface? Although numerical modeling of the diffusion with different translation-rotation couplings to answer this question was desirable, this is not feasible at present. DFT calculations of CO on metal surfaces have been a long-standing challenge [31,32], and it is not possible to stabilize a CO dimer on Ag(100) with state-of-the-art methods [29]. However, there are two indications that the influence of the stronger binding of the immobile CO molecule to the Cu atom hardly changes the energetics of the CO dimer rotation. First, the CO—CO binding energy is only weak; see above. Second, dimers separate into monomers at a similar temperature on both surfaces, pointing to a similar binding.

Our results thus suggest that the additional degree of freedom gained by dimerization is at the origin of the larger dimer mobility. This conclusion is supported by statistics of the different types of motion for the dimer on the elemental surface [Fig. 4(c)]. At all three temperatures, the sum of all events showing a change in orientation amounts to approximately 60%, while the pure diffusion events amount to 40%. Thereby, the number of purely rotational events decreases at higher temperature, as expected. The number of rotations around the center, which cannot lead to any center-of-mass diffusion, amounts to approximately 20% at low temperature. If we disregard this number, around the same amount of molecules are and are not changed in orientation, supporting our interpretation that the diffusion consists of subsequent rotation events.

The analysis presented in Fig. 4(c) might also explain why D_{110} is never observed on the elemental Ag(100). In the intermediate state, the repulsion of the two CO molecules pushes the other molecule to the next adsorption site, which in half of the cases will lead to the rotation
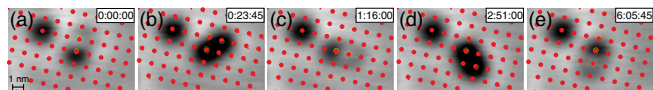

FIG. 5. Kinetics of CO dimer on Cu/Ag(100): (a–e) Snapshot of a movie (80 images, $\Delta t = 285$ s, 16.0 K) at indicated times in h:min:s; dots correspond to on-top surface sites determined from full image; dashed circles give positions of depressions determined via Gaussian fits (20 pA, 50 mV).

around the center of mass. The molecule on the Cu, in contrast, is too strongly bound to be pushed away, leading to stabilization of the intermediate state. This implies that the Cu has changed the potential landscape, however, not markedly enough to change the barrier for rotational motion beyond the experimental error.

Our result may explain the other observed diffusivity enhancements upon dimer formation. For CO dimers on Cu(110) [5], the dimers consisting of two molecules on adjacent rows may rotate by changing between D_{100} and D_{112} with the former being the more stable dimer imaged by STM. The motion of water dimers on Pt(111) includes a rotational motion around one of the molecules following the abovementioned hydrogen bond rearrangements including tunneling [8]. Note that the rotational motion does not need to be 45° for the dimer of the much larger molecule tetra-pyridylporphyrin on Cu(111) [7], as intermediate angles might lead to stable adsorption orientations. In contrast, tunneling-electron-induced rotation of oxygen molecules on Pt(111) cannot lead to diffusion, as the rotating molecule is trapped with one atom in a hollow site, and only the other molecule changes between almost on-top site positions [33]. Likewise, the hexa-tert-butyl decacyclene at close-to-monolayer coverage rotates on Cu(100) only around its center, as it could not diffuse due to space limitations [34].

In general, alternating rotation of one of the molecules around the other one, acting as anchor point, leads to a diffusion that accelerates the overall mass transport, as demonstrated here for CO on Ag(100). Our result is supported by a recent DFT study for Co phtalocyanine on Ag(100) that revealed the importance of rotational motion in diffusion of this extended molecule [14].

In conclusion, our study shows that the enhanced diffusivity of a dimer on the elemental surface results from a rotational motion; i.e., dimer rotation leads to long-range fast diffusivity. In other words, the additional degree of rotational freedom leads to an increased diffusivity, a process that is likely to be relevant for other molecules that form dimers and will thus influence all surface processes that involve diffusion at realistic coverages.

As an example, we discuss the implication of our results for heterogeneous catalysis. Despite similarities in motion, the overall contribution of dimers to mass transport, the rate limiting step in heterogeneous catalysis, is markedly different on the two surfaces. The diffusion barrier of CO dimers

is only about 70% of the one of monomers on Ag(100). Dimer formation on Ag(100) thus increases the diffusivity of the molecules by orders of magnitude. In contrast, dimer formation on the alloy traps CO and limits its motion to the immediate vicinity of the Cu-adsorbed CO. This would be advantageous if the two molecules were the different reactants. If, however, both molecules were of the same species that have to diffuse to their reaction sites, it would be the elemental surface that enhances the turnover rate. Beyond this specific example, concerted diffusion of weakly interacting molecules affects other fields in nanoscience, which involve material transport as supramolecular architectures or nanoparticle growth.

[1] G. Antczak and G. Ehrlich, *Surface Diffusion: Metals, Metal Atoms, and Clusters* (Cambridge University Press, New York, 2010), and citations therein.

[2] F. Rosei, M. Schunack, Y. Naitoh, P. Jiang, A. Gourdon, E. Lægsgaard, I. Stensgaard, C. Joachim, and F. Besenbacher, Prog. Surf. Sci. **71,** 95 (2003).

[3] P. Jensen, Rev. Mod. Phys. **71,** 1695 (1999).

[4] S. E. Shore, J.-P. Ansermet, C. P. Slichter, and J. H. Sinfelt, Phys. Rev. Lett. **58,** 953 (1987); K. D. Dobbs and D. J. Doren, J. Chem. Phys. **97,** 3722 (1998); T. Mitsui, M. K. Rose, E. Fomin, D. F. Ogletree, and M. Salmeron, Phys. Rev. Lett. **94,** 036101 (2005); K. Stepan, J. Güdde, and U. Höfer, Phys. Rev. Lett. **94,** 236103 (2005); E. H. G. Backus, A. Eichler, A. W. Kleyn, and M. Bonn, Science **310,** 1790 (2005); M. Mehlhorn, H. Gawronski, and K. Morgenstern, Phys. Rev. Lett. **104,** 076101 (2010); Ch. Zaum, K. M. Meyer-auf-der-Heide, M. Mehlhorn, S. McDonough, W. F. Schneider, and K. Morgenstern, Phys. Rev. Lett. **114,** 146104 (2015).

[5] B. G. Briner, M. Doering, H.-P. Rust, and A. M. Bradshaw, Science **278,** 257 (1997).

[6] T. Mitsui, M. K. Rose, E. Fomin, D. F. Ogletree, and M. Salmeron, Science **297,** 1850 (2002).

[7] M. Eichberger, M. Marschall, J. Reichert, A. Weber-Bargioni, W. Auwärter, R. L. C. Wang, H. J. Kreuzer, Y. Pennec, A. Schiffrin, and J. V. Barth, Nano Lett. **8,** 4608 (2008).

[8] V. A. Ranea, A. Michaelides, R. Ramirez, P. L. de Andres, J. A. Verges, and D. A. King, Phys. Rev. Lett. **92,** 136104 (2004).

[9] M. Schunack, T. R. Linderoth, F. Rosei, E. Læ gsgaard, I. Stensgaard, and F. Besenbacher, Phys. Rev. Lett. **88,** 156102 (2002).

[10] J. S. Raut and K. Fichthorn, J. Vac. Sci. Technol. A **15,** 1542 (1997).

[11] J. Weckesser, J. V. Barth, and K. Kern, Phys. Rev. B **64,** 161403 (2001).

[12] W. D. Luedtke and U. Landman, Phys. Rev. Lett. **82,** 3835 (1999).

[13] T. Yokoyama, T. Takahashi, and K. Shinozaki, Phys. Rev. B **82,** 155414 (2010).

[14] G. Antczak, W. Kaminski, A. Sabik, C. Zaum, and K. Morgenstern, J. Am. Chem. Soc. **137,** 14920 (2015).

[15] M. Mehlhorn, H. Gawronski, L. Nedelmann, A. Grujic, and K. Morgenstern, Rev. Sci. Instrum. **78,** 033905 (2007).

[16] A. Beichert, Ch. Zaum, and K. Morgenstern, Phys. Rev. B **92,** 045422 (2015).

[17] C. Zaum, C. Bertram, K. M. M. auf der Heide, M. Mehlhorn, and K. Morgenstern, Rev. Sci. Instrum. **87,** 053902 (2016).

[18] See Supplemental Material at http://link.aps.org/supplemental/10.1103/PhysRevLett.121.185901, which gives further experimental details and explains the identification of monomer and dimer on the elemental surface and of the diverse dimers on the surface alloy and which includes Refs. [1,15–17,19–22].

[19] E. Ganz, S. K. Theiss, I.-S. Hwang, and J. Golovchenko, Phys. Rev. Lett. **68,** 1567 (1992); Y. W. Mo, Phys. Rev. Lett. **71,** 2923 (1993); J. Repp, F. Moresco, G. Meyer, K.-H. Rieder, P. Hyldgaard, and M. Persson, Phys. Rev. Lett. **85,** 2981 (2000); G. Meyer, L. Bartels, S. Zöphel, and K.-H. Rieder, Appl. Phys. A **68,** 125 (1999); M. Forsblom and M. Persson, J. Chem. Phys. **127,** 154303 (2007); J. A. Nieminen, E. Niemi, and K.-H. Rieder, Surf. Sci. **552,** L47 (2004); A. van der Pol, A. van der Avoird, and P. E. S. Wormer, J. Chem. Phys. **92,** 7498 (1990); A. J. Heinrich, C. P. Lutz, J. A. Gupta, and D. M. Eigler, Science **298,** 1381 (2003); M. Mehlhorn, H. Gawronski, and K. Morgenstern, Phys. Rev. Lett. **104,** 076101 (2010).

[20] C. Zaum, M. Rieger, K. Reuter, and K. Morgenstern, Phys. Rev. Lett. **107,** 046101 (2011); C. Zaum, J. Meyer, K. Reuter, and K. Morgenstern, Phys. Rev. B **90,** 165418 (2014).

[21] M. Persson, Phil. Trans. R. Soc. A **362,** 1173 (2004).

[22] A. van der Pol, A. van der Avoird, and P. E. S. Wormer, J. Chem. Phys. **92,** 7498 (1990).

[23] G. Boisvert and L. J. Lewis, Phys. Rev. B **56,** 7643 (1997).

[24] D. W. Bassett, J. Phys. C **9,** 2491 (1976).

[25] G. L. Kellogg, T. T. Tsong, and P. Cowan, Surf. Sci. **70,** 485 (1978).

[26] P. J. Feibelman, Phys. Rev. Lett. **58,** 2766 (1987).

[27] K. Morgenstern, K.-F. Braun, and K. H. Rieder, Phys. Rev. Lett. **93,** 056102 (2004).

[28] E. Niemi and J. Nieminen, Chem. Phys. Lett. **397,** 200 (2004).

[29] A. Azur, E. Pollak, M. Jørgensen, and H. Grönbeck (private communication).

[30] M. L. Anderson, N. C. Bartelt, P. J. Feibelman, B. S. Swartzentruber, and G. L. Kellog, Surf. Sci. **600,** 1901 (2006); Z. Chen, N. Kioussis, K.-N. Tu, N. Ghoniem, and J.-M. Yang, Phys. Rev. Lett. **105,** 015703 (2010).

[31] Q.-M. Hu, K. Reuter, and M. Scheffler, Phys. Rev. Lett. **98,** 176103 (2007).

[32] P. Lazic, M. Alaei, N. Atodiresei, V. Caciuc, R. Brako, and S. Blügel, Phys. Rev. B **81,** 045401 (2010).

[33] B. C. Stipe, M. A. Rezaei, and W. Ho, Science **279,** 1907 (1998).

[34] J. K. Gimzewski, C. Joachim, R. R. Schlittler, V. Langlais, H. Tang, and I. Johannsen, Science **281,** 531 (1998).